Periocular Region Appearance Cues for Biometric Identification

Damon L. Woodard Shrinivas J. Pundlik Jamie R. Lyle Philip E. Miller
Biometrics and Pattern Recognition Lab, School of Computing
Clemson University, Clemson, SC 29634 USA
{woodard, spundli, jlyle, pemille}@clemson.edu

Abstract

We evaluate the utility of the periocular region appearance cues for biometric identification. Even though periocular region is considered to be a highly discriminative part of a face, its utility as an independent modality or as a soft biometric is still an open ended question. It is our goal to establish a performance metric for the periocular region features so that their potential use in conjunction with iris or face can be evaluated. In this approach, we employ the local appearance based feature representation, where the image is divided into spatially salient patches, and histograms of texture and color are computed for each patch. The images are matched by computing the distance between the corresponding feature representations using various distance metrics. We report recognition results on images captured in the visible and near-infrared (NIR) spectrum. For the color periocular region data consisting of about 410 subjects and the NIR images of 85 subjects, we obtain the Rank-1 recognition rate of 91% and 87% respectively. Furthermore, we also demonstrate that recognition performance of the periocular region images is comparable to that of face.

1. Introduction

In recent years, face and iris have established themselves as widely popular modalities for human identification [4, 23]. Despite the recent advances, the performance of iris and face recognition algorithms declines when dealing with non-ideal scenarios such as non-uniform illumination, pose variations, occlusions, expression changes, and radical appearance changes in the input images. These challenges can be tackled either by: i) improving the existing algorithms that handle various aspects of the recognition problem, ii) combining multiple complementary modalities, or iii) exploring newer traits that can perform or aid the process of recognition. Periocular region has potential to be such a trait, as it is considered to be one of the highly discriminative regions of a face [19]. In this paper, our goal is to explore various appearance based cues that can be extracted from the region surrounding the human eye and evaluate their utility to perform identification, independent of other modalities. The eventual goal of this empirical study is to establish techniques that use periocular region appearance features to help iris and face recognition algorithms.

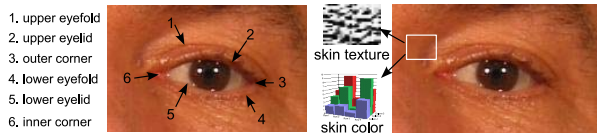

Figure 1. Some key periocular region features. LEFT: Level-one features that are mostly geometric in nature. RIGHT: Level-two features, like skin texture and color can be extracted from the area surrounding the eye.

The periocular region is a small region in the neighborhood of the eye and may include eyebrows. Its use for identification or verification predominantly figures in the case of approaches that are based on iris [6], vein patterns of the eye[5], or partial facial features [9, 8, 7, 18, 22]. A recent approach performs identification solely based on the periocular region texture features [15]. While iris or retinal pattern based identification relies only on the specific information found within the eye, approaches dealing with face recognition using partial facial features consider the entire eye region as one of the many discriminative features. Though they differ in terms of how a periocular region is precisely defined, the above mentioned approaches dealing with partial facial features conclude that the periocular region is superior as compared to other salient facial regions such as nose or mouth, for identification. Apart from this, our motivation for using the information present in the periocular region also stems from the fact that periocular region is the common link between face and iris based recognition, and can potentially aid both these modalities.

Traditional iris recognition algorithms are based on encoding and matching the iris texture pattern [6], but are sensitive to the quality of the iris images. This is especially true in the case of images captured in the visible spectrum.

Combining the discriminative information gathered around the eye with iris features has the potential to improve the overall recognition performance. Similarly, in the context of facial recognition, the use of periocular region may be beneficial in situations where the face is partially occluded, or the subjects have facial hair, etc. Also, it has been proposed in some recent approaches that part-based face representation [1, 8, 9], as opposed to the traditional holistic face representation [2, 21], may lead to improved face recognition performance. Of the various facial components, eyes and the region surrounding them is known to be highly discriminative [18]. In this regard, it would be noteworthy to study the effect of features extracted from the periocular region on face recognition in greater detail.

Some of the prominent periocular region features are shown in Figure 1. Excluding the iris, these features can be classified as level one-features that include both upper and lower eyelids, eye folds, and eye corners; or level-two features such as detailed skin texture, fine wrinkles, color, or skin pores. Level-one features tend to be more dominant in nature as compared to the level-two features. Alternatively, the features can also be classified based on geometry (shape of the eye, eye lids, eye folds and various lines), texture, or color. Again, most of the level-one features fall into the category of geometric features (shape dependent), while level-two features can be classified as texture or color features.

In this paper we demonstrate that low-level features extracted from the periocular region can be effectively used for identification. As compared to the previous approaches dealing with periocular region such as [15], the chief novelty in this work lies in our use of only the level-two periocular features based on skin texture and color information (if available) to perform identification. To this effect, we mask the eye in the periocular region (see Figure 4) thus removing the iris and various level-one features. The reason for such an exclusion is that it eliminates the effect of iris on the computed texture and color features, thus facilitating a way to compute unbiased recognition performance metric for the periocular region features. Although removal of the eye from a periocular region image may seem like a heavy loss of discriminating information, it could be potentially advantageous as the level-one features are highly sensitive to the opening and closing of the eyes and may end up influencing the texture features adversely (as they are very dominant due to relatively high gradients). We show recognition results using color periocular images extracted from the Facial Recognition Grand Challenge (FRGC) II [17] dataset. Furthermore, we demonstrate the recognition results using the near-infrared (NIR) periocular images extracted from the Multiple Biometrics Grand Challenge (MBGC) [16] NIR face videos. We are not aware of any other approach that has used the NIR periocular region images. For further validation, we show that the recognition results obtained from the color periocular region compare favorably with those obtained using full face images. The subsequent sections describe the details of our approach and the experimental results.

Figure 2. Different ways of extracting periocular regions from face images. For this work, non-overlapping regions for the left and the right eyes are extracted.

2. Periocular Region Data

One of the ways to obtain periocular region images is to extract them from face images. Different schemes of extracting periocular region images from face images are shown in Figure 2 that include cropping the entire strip containing both the eyes, or extracting two overlapping regions corresponding to both. In this work, we extract two distinct non-overlapping images belonging to each left and right eye. Since one of our eventual goals is to combine information obtained from the periocular region with the iris texture, and since iris images are typically captured separately for each eye, such an independent handling of both the periocular regions would facilitate efficient information fusion between the two modalities. The size of the extracted periocular region images is another consideration. Ideally, the periocular region image should be such that it captures the region around the eye in sufficient detail, while not compromising on the size (or quality) of the iris region. Increasing the image size can lead to increased discriminative ability only up to a certain extent because as the periocular image becomes larger in size, a larger number of pixels belonging to the forehead or cheek region would form part of it. Operating under these constrains, we extract the color and NIR periocular region images from the face images as described below.

2.1. Color Periocular Region Images

The color periocular region data used in the experiments described in this paper are extracted from the frontal face images present in the FRGC database [17]. The FRGC database consists of high resolution color images ($\approx$ 1200×1400, 72 dpi) of a large number of subjects mostly between ages 18 and 22, collected over a two year period from multiple recording sessions involving controlled and uncontrolled lighting conditions, and with and without expressions (neutral expression). In controlled conditions, the

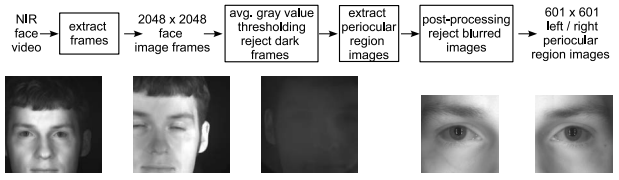

Figure 3. TOP ROW: Steps for obtaining NIR periocular region images from the MBGC NIR face video data. BOTTOM ROW: Some examples of face image frames extracted from a MBGC NIR face video, along with the periocular region images corresponding to the first example frame. Notice that not all the frames in the video are usable.

distance between the subjects and the camera is approximately the same. The FRGC dataset was chosen for this work because of the availability of high resolution face images which would lead to relatively larger periocular region images. This would enable us to perform iris recognition in the visible spectrum in the future. Moreover, periocular color and texture information can be captured reliably from the high resolution images.

The ground truth eye centers for the faces are provided in the FRGC dataset which act as the centers of the periocular images to be cropped out of the original face images. The size of the cropping region is calculated by a ratio of the distance between the eye centers. The periocular region images are then scaled down to a uniform size of 100x160 pixels. These extracted images, as compared to the original facial image, are shown in Figure 2. For computing texture, the images are converted to grayscale and preprocessed by histogram equalization. For color image preprocessing, the RGB image is converted to the CIE L*a*b* color space, the luminance channel histogram is equalized, and then converted back to the RGB color space. These steps are followed in order to preserve the color information. To eliminate the effect of texture and color in the iris and the surrounding sclera area, an elliptical mask of neutral color is placed over the center of the periocular region image. The dimensions of the ellipse are predefined based on the dimensions of the input periocular image rather than the dimensions of the subjects' eye. The underlying assumption (based on empirical study of the data that we are using) is that the change in size of the eye is mostly on account of its varying amount of opening and not so much due to changes in scale. This, coupled with the fact that the images are aligned and scaled to a fixed size, allows placing of a fixed size ellipse on the eye such that a significant amount of periocular skin is still visible.

2.2. NIR Periocular Region Images

The NIR periocular region data used in this paper are extracted from frontal face videos that form a part of the

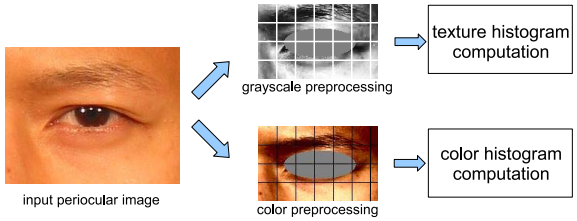

Figure 4. Overview of the steps for computing texture and color representation of a periocular region image.

MBGC portal challenge, where the subjects walk through a portal that captures videos of the face (both the visible and NIR spectrum) and iris (NIR). The goal of the MBGC dataset is to perform recognition using multiple modalities of face and iris (still images and videos). The NIR iris video and still images are not suitable for this work as very little periocular region is visible. Hence, we use the NIR face videos and extract periocular regions to construct our test dataset.

The videos range from 15 to 30 frames in length and consist of 2048×2048 images of varying quality (see Figure 3). The variation in the image quality is on account of the NIR lights shining only for a brief duration of the time as the subject walks through the portal. This causes some frames to be too dark or too bright. Other effects such as blinking, partial occlusion of the face, motion blur, etc. are also present in a large number of frames. In order to process these videos, we employ the steps shown in Figure 3. The images extracted from the video are thresholded based on their average grayscale value so as to reject those frames in which the face is not visible. Then the eye centers are marked and periocular regions of size 601×601 are extracted. Even though there is some scale change in the face as the subject walks toward the camera, most of the usable frames (higher quality) are in the earlier part of the video, where the scale change is not substantial. For this reason, the effects of scale change are ignored and a fixed sized periocular region image centered at the eye is extracted. To remove blurred images, high frequency content is measured from the 2D Fourier spectrum obtained by convolving the image with a 8×8 kernel. A threshold is set for each subject based on the maximum and the minimum energy obtained from processing all the frames belonging to the subject. Rejecting the blurred images results in a set of usable left and right periocular region images used for the experiments presented in section 4.

3. Periocular Region Features

As described earlier, in this work we match two periocular region images using level-two periocular region features. In case of the images from visible spectrum, we use both skin texture and color, while for the NIR periocular

region images, only texture is used. Use of skin texture for recognition has been investigated from various perspectives. While some approaches explicitly use the so called skin micro-features such as moles, scars, or freckles [10], others adopt a more general representation for the overall texture in the periocular region using popular texture measures such as discrete cosine transform (DCT) [7], gradient orientation histogram (GOH, or alternatively known as Histograms of Oriented Gradients), or local binary patterns (LBP) [13, 15]. Usually, these popular texture measures are used for computing the texture locally, and the entire image is represented as a combination of these local texture features, thus leading to the idea of local appearance features. To this effect, we divide the periocular region image into blocks and locally compute the texture and color features (see Figure 4). A texture or color feature vector describing the entire image is then computed by concatenating the vectors corresponding to the each of the blocks. Such a local appearance based representation is well suited for this work because it preserves the spatial relationship of the features. As our input images are aligned and normalized (for size), it is easier to partition the images into blocks. This leads to a fixed length feature vector for each image that can be directly used for matching without any further normalization of the vector.

Let I be the preprocessed input periocular region image (color, I_c or grayscale, I_t depending on the data) divided into N blocks of M pixels each with $I^{(i)}$ representing the i^{th} image block, then the texture feature representation of the image is given by an ordered set $\mathscr{T}(I_t) = \left\{T^{(1)}, \ldots, T^{(N)}\right\}$, where $T^{(1)}, \ldots, T^{(N)}$ are the texture histograms corresponding to the N blocks. Similarly, the color feature representation of the image is given by $\mathscr{C}(I_c) = \left\{C^{(1)}, \ldots, C^{(N)}\right\}$, with $C^{(1)}, \ldots, C^{(N)}$ being the color histograms of the N blocks. Details of our color and texture feature implementations are described below.

3.1. Skin Texture

We use the local binary patterns (LBPs) as the periocular texture measure. Local Binary Patterns (LBP) [14] quantify intensity patterns found in local pixel neighborhood patches and are useful for identifying spots, line ends, edges, corners, and other distinct texture patterns. Their use is popular in various biometric applications such as face recognition [1, 11], facial expression recognition [12], and iris recognition [20].

We now briefly describe the computation of LBP histogram for an image. For a more detailed description of LBP, see [14]. As the name suggests, computing a LBP score for a pixel involves counting the binary changes of intensity patterns in a p pixel neighborhood along a circle of radius r around that pixel. Subtracting the intensity of the center pixel from its neighbors and using the sign of the difference instead of the actual difference leads to illumination and scale invariance in the local neighborhood. Each pixel intensity change is assigned a binomial weight to obtain a binary code for the local neighborhood. If $\mathbf{x}_j^{(i)}$ represent the coordinates of the j^{th} pixel of the i^{th} block, then the LBP vector at this pixel location is given by

$$\widetilde{\phi}\left(\mathbf{x}_j^{(i)}\right) = \sum_{k=0}^{p-1} s\left(I_t(\mathbf{x}_k^{(i)}) - I_t(\mathbf{x}_j^{(i)})\right) 2^p, \qquad (1)$$

where $s(.)$ is the sign operator, p is the number of pixels in the local neighborhood of $\mathbf{x}_j^{(i)}$, and $I_t(\mathbf{x}_k^{(i)})$, $I_t(\mathbf{x}_j^{(i)})$ represent intensities at locations $\mathbf{x}_k^{(i)}$, and $\mathbf{x}_j^{(i)}$ respectively. The above equation results in 2^p dimensional vector for each pixel corresponding to the 2^p binary patterns found in the p pixel neighborhood of a pixel. The number of bitwise changes in the pattern obtained in a pixel neighborhood is called the uniformity measure and is denoted by $U\left(\widetilde{\phi}\left(\mathbf{x}_j^{(i)}\right)\right)$. In this work, we use the uniformity value of 2 leading to a LBP vector

$$\phi\left(\mathbf{x}_j^{(i)}\right) = \begin{cases} \sum_{k=0}^{p-1} s\left(I_t(\mathbf{x}_k^{(i)}) - I_t(\mathbf{x}_j^{(i)})\right), & \text{if } U\left(\widetilde{\phi}\left(\mathbf{x}_j^{(i)}\right)\right) \leq 2 \\ p+1, & \text{otherwise} \end{cases}$$

where

$$\begin{aligned} U\left(\widetilde{\phi}\left(\mathbf{x}_j^{(i)}\right)\right) &= \left|s\left(I_t(\mathbf{x}_{p-1}^{(i)}) - I_t(\mathbf{x}_j^{(i)})\right) - s\left(I_t(\mathbf{x}_{k-1}^{(i)}) - I_t(\mathbf{x}_j^{(i)})\right)\right| \\ &+ \sum_{k=1}^{p+1} \left|s\left(I_t(\mathbf{x}_k^{(i)}) - I_t(\mathbf{x}_j^{(i)})\right) - s\left(I_t(\mathbf{x}_{k-1}^{(i)}) - I_t(\mathbf{x}_j^{(i)})\right)\right|. \end{aligned}$$

An LBP vector is computed for each pixel in an image patch $I^{(i)}$, which is in turn encoded into a histogram of bins $b_t = p(p-1)+3$ given by:

$$T^{(i)} = hist\left(\left\{\phi\left(\mathbf{x}_1^{(i)}\right), \ldots, \phi\left(\mathbf{x}_M^{(i)}\right)\right\}, b_t\right). \qquad (2)$$

The dimensionality of this patch histogram results from the fact that there are $p-1$ uniform patterns for each of the p bit changes and an addition bit change. The 3 remaining bins store the 2 uniform patterns where uniformity value is 0, and all non-uniform patterns. Our implementation sets $r = 1$ and $p = 8$, resulting in a 59 bin histogram for a 3×3 neighborhood.

3.2. Color Features

Color histogram based representation of the periocular region images can be computed in various color spaces. We experiment with the RGB and HSV color spaces and their sub-spaces. In case of RGB images, it is common to consider all three color channels for histogramming (3D histogram). But we observed that using only two channels instead of three for histogram construction (2D histogram)

gave a comparable performance while being more efficient. Let I_c be the preprocessed color periocular image. Like texture computation, color histograms are computed for each image block $I_c^{(i)}$ and are given by $C^{(i)} = hist\left(\psi(I_c^{(i)}), b_c\right)$, where $\psi(I_c^{(i)})$ is the transformation of a RGB image into either a different color space or a sub-space, and b_c is the number of bins. We experimented with RB, RG, GB and HSV color spaces and found that RG color space outperforms the others. Of the various bin configurations that we tried, the 4×4 histogram (with $b_c = 16$) performed better than both coarser and finer binning configurations.

3.3. Matching Periocular Region Features

Matching of two images is done by computing the distance (or similarity) metric using the corresponding feature representations. For the FRGC dataset, we perform score level fusion for the texture and color representations ($\mathscr{T}(I_t)$, $\mathscr{C}(I_c)$ respectively) and hence, both can be separately matched for a pair of images. For matching, $\mathscr{T}(I_t)$ and $\mathscr{C}(I_c)$ are converted to their vectorized forms $\overline{\mathscr{T}}(I_t)$ and $\overline{\mathscr{C}}(I_c)$ of $N \times b_t$ and $N \times b_c$ dimension respectively. We set $N = 28$ for the color periocular region images, while for NIR images, $N = 36$. A function $D\left(\overline{\mathscr{T}}(I_{t,pr}), \overline{\mathscr{T}}(I_{t,gl})\right)$ compares the texture features for the probe and gallery images ($I_{t,pr}$ and $I_{t,gl}$). Similar convention is followed in the case of color images. We experiment with various commonly used histogram comparison functions such as L1, L2 norm, correlation, covariance, cityblock distance, Jefferey divergence, chi-squared distance, Bhattacharya coefficient, and histogram intersection. In the case of LBP texture features, cityblock performs the best while in the case of color histograms Bhattacharya coefficient outperforms the others. The color and texture are combined at the match score level (distance or similarity values) using summing with min-max normalization. For all the experiments, we weigh both color and texture equally, although texture could be given a higher weight as it gives better recognition on its own.

4. Experimental Results

The experimental set of color periocular region images comes from the face images captured under controlled lighting that constitute the original FRGC Experiment 1. Two images per subject are used as a gallery set that come from the neutral expression face images captured in the same session. The three experiments, named *FRGC-1*, *FRGC-2*, and *FRGC-3* are differentiated by their probe images. *FRGC-1* contains one neutral expression image from each subject from a different recording session, *FRGC-2* is composed of alternate expression images from the same recording session, and *FRGC-3* has alternate expression images from a different recording session. Each of these experiments have sub-experiments using only left eyes, only right eyes, and a fusion of both eyes (score-level fusion with min-max normalization). Additionally, we use the full face images in each of these experiments for the purpose of comparing the recognition rates obtained using the periocular region. The idea of local appearance based recognition that was applied while computing the periocular features is also used in the case of face recognition, i.e., the face image is divided into blocks, and features are computed and matched for each block. The preprocessing of the face images is done using the approach detailed in [3] resulting in 195×225 facial images that are divided in 49 blocks. Of the 466 test subjects in the original FRGC dataset, there are 410 subjects that have images taken in multiple recording sessions, resulting in a total of 4100 (2050 for each region, 3 probe, 2 gallery) periocular region images for all three experiments combined.

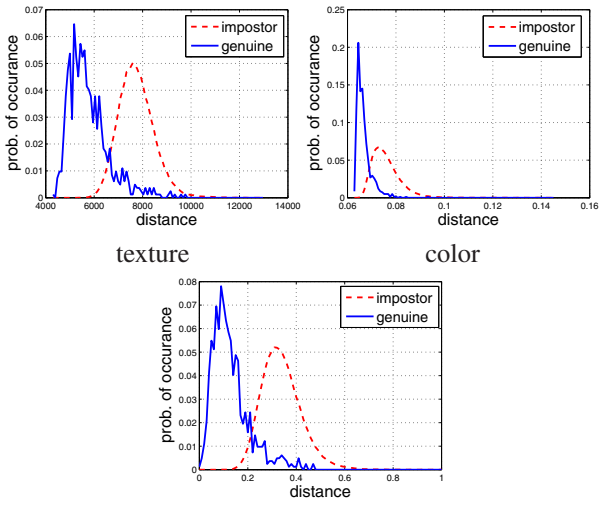

Figure 5. Genuine and impostor score distribution for the left periocular region images for *FRGC-1* experiment.

Figure 5 shows the match score distribution for the texture and color features for the left periocular region of *FRGC-1*, emphasizing the relatively higher discriminative ability of the texture based representation as compared to the color based representation. Similar distribution is observed for the right periocular region. Figure 6 shows the Cumulative Match Characteristics (CMC) for the left, right, and combined left and right periocular regions for *FRGC-1* and *FRGC-3* experiments using texture, color, and a fusion of both. The joint Rank-1 recognition rates obtained using both right and left periocular regions are consistently higher for the texture and color as compared to those using only either left or right. The combined texture and color recognition is higher as compared to their individual recognition, except in the case of joint left and right periocular region for *FRGC-1* experiment, where the relatively lower recognition rates of color features as compared to texture bring down

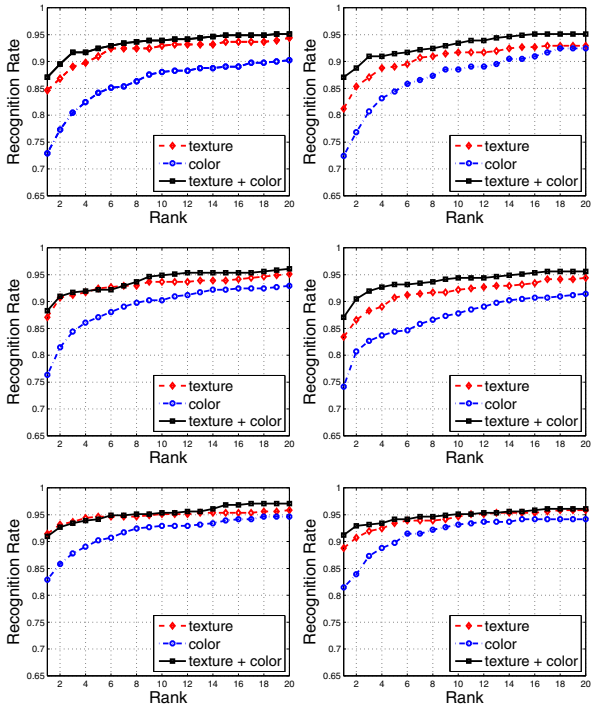

FRGC-1 *FRGC-3*

Figure 6. Cumulative Match Characteristics for the experiments *FRGC-1* (left) and *FRGC-3*(right) on the left, right and left + right (top to bottom) using texture, color, and combination of both.

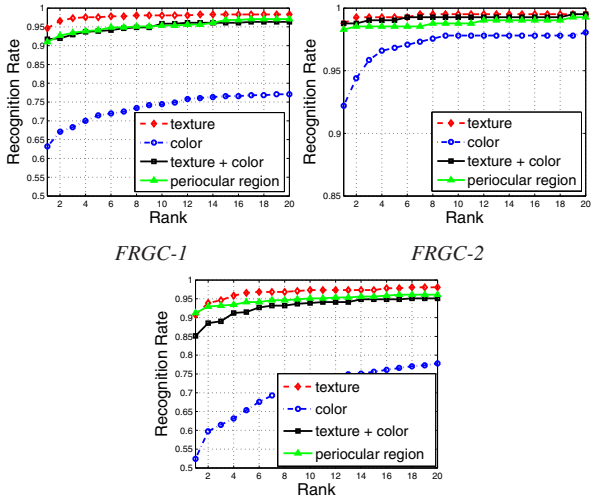

FRGC-1 *FRGC-2*

FRGC-3

Figure 7. Cumulative Match Characteristics for the experiments *FRGC-1*, *FRGC-2*, and *FRGC-3* using full face image.

the overall recognition rates. A similar trend is observed in the case of the recognition using full face images (see Figure 7). The main reason that the color cannot perform well in the case of the face images is that there is more intra-class variability in the case of the face images due to slight illumination changes or presence of facial hair, as compared to the periocular images. When comparing neutral to alternate expression faces, in addition to the above problems, expression change can cause the mouth (and teeth) to span different blocks, thus degrading the color histograms performance for face recognition in the *FRGC-3* experiment. For *FRGC-2* experiment, since the images were captured in the same session, the similarity of the color information outweighs the differences caused by expression in the face, resulting in higher recognition rates for the face and periocular regions. Table 1 summarizes the Rank-1 recognition rates for all experimental configurations.

It can be observed from Table 1 that the recognition rate drops off across the board when using probe images from different sessions and this factor is more prominent than the expression change in affecting the recognition rates. It can also be seen that recognition obtained using only the periocular region is comparable to that obtained using the entire face. In the current experimental setting, the texture and color representation of periocular regions are less influenced by expression change as there is only a slight drop in their recognition performance (*FRGC-1* vs. *FRGC-3*). In some cases, the combined texture and color representation for the periocular regions outperform the face. Our goal is not to claim that periocular region is superior to the face, but to merely point out that in certain situations, periocular regions alone is sufficient for accurate recognition. There may be certain situations, such as illumination changes, that affect the periocular region features drastically and in such cases, using the entire face would lead to a better performance. We cannot directly compare the results obtained in this work to some of the previous works due to the differences in the datasets used or due to the differences in the experimental setup. But as compared to [7] that uses FRGC Experiment 1 images (P2 partitioning, F1 experimental set, left eye ≈90 %, right eye ≈88%), we obtain similar recognition results. But it should be noted that in their case, the experimental setup is not clearly defined and the number of subjects involved in testing is much less than ours. Also, we are using the information strictly around the eye and no information inside the eye is utilized. This indicates the highly discriminative nature of the periocular region texture and color features.

The NIR periocular region dataset consists of videos of 115 subjects with 2-20 usable face images per subject leading to over 1700 face images. Of these, not all have both right and left eyes visible, thus leading to 85 subjects, 689 right periocular region images, and 113 subjects, 911 images for the right and left periocular region images respectively. Many of these images are of very low quality as described in Section 2.2. We retain the first two images of the video as gallery images, while choosing a probe image at random from the remaining useful frames for that subject. The left and the right periocular region are compared sepa-

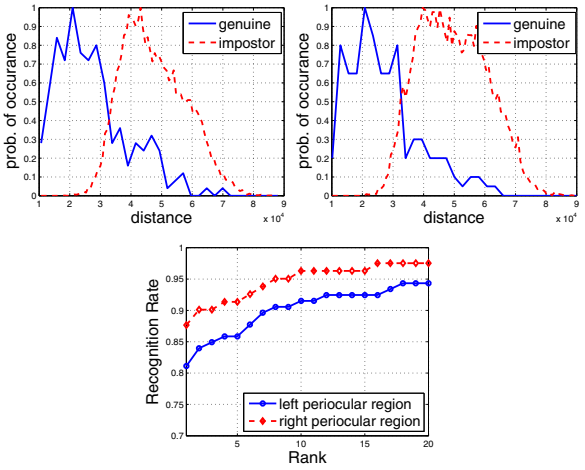

Figure 8. Genuine and impostor score distribution for the (a) left, (b) right periocular region images for MBGC NIR experiment along with the CMC for both (c).

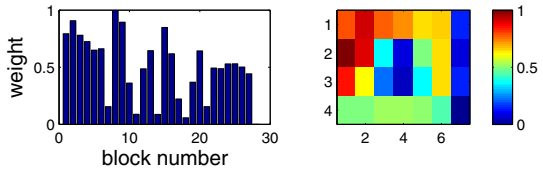

Figure 9. The discriminative ability of each local block in the periocular region. The plot (left) and the weight map (right) is shown for *FRGC-1* right region using texture.

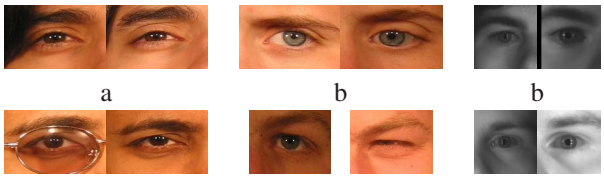

Figure 10. Some examples pairs of gallery (left) and probe (right) images of the same subjects from both the FRGC and MBGC NIR datasets that failed to match.

rately, giving the Rank-1 recognition rates of 81% and 87% respecively. Figure 8 shows the score distribution and the CMC statistics for the NIR periocular images. The separability of the genuine and the impostor scores as well as the Rank-1 recognition rate is lower in the case of NIR images as compared to the color images due to the poor quality of the NIR data. Still, these statistics indicate that periocular region when used with iris may provide some boost to the overall recognition rate.

Relative discriminative ability of each image block for *FRGC-1* left eye using texture is shown in Figure 9. The center of the eye receives lowest weight due to the presence of the mask while the blocks on the periphery (especially the top ones as they represent the eyebrows) are highly discriminative. Figure 10 shows some examples where the probe image failed to match with the gallery images. In case of the FRGC images, the main reasons for failure to match are occlusion of the periocular region (Figure 10a), presence of glasses (Figure 10d), or radical appearance changes (Figure 10e). Another cause is the misalignment of the images Figure 10b). Since the ground truth eye centers are located on the center of the pupil, movement of the eye shifts the center and consequently affects the cropped periocular region. In the case of the NIR images, blurring and scale change is the most likely cause of a non-match. Another reason is the illumination changes caused due to the NIR lighting leading to washout of the images.

5. Conclusion

This paper investigates the utility of various appearance cues such as periocular skin texture and color for biometric identification. The experiments presented in this paper measure the performance of this new biometric on color and near-infrared periocular region image data. The recognition rates obtained by the periocular region are comparable to those obtained by using the full face using similar features based on local appearance. The experiments presented in the paper demonstrate that at its best, the periocular region holds a lot of promise as a novel modality for identifying humans with a potential of influencing other established modalities based on iris and face. At the very least, the results suggest a potential for using periocular region as a soft biometric. Future work includes evaluation of more periocular features, comparison of periocular based recognition performance to a commercial face recognition algorithm, exploration of how the capture conditions and the image quality such as uncontrolled lighting, or subjects wearing cosmetics affect the periocular skin texture and color, among others

References

[1] T. Ahonen, A. Hadid, and M. Pietikainen. Face description with local binary patterns: application to face recognition. *IEEE Transactions on Pattern Analysis and Machine Intelligence*, 28(12):2037–2041, 2006.

[2] P. N. Belhumeur, J. P. Hespanha, and D. J. Kriegman. Eigenfaces vs. fisherfaces: recognition using class specific linear projection. In *Proceedings of the European Conference on Computer Vision*, pages 45–58, 1996.

[3] J. Beveridge, D. Bolme, B. Draper, and M. Teixeira. The csu face identification evaluation system: Its purpose, features, and structure. *Machine Vision and Applications*, 14(2):128–138, 2006.

[4] K. Bowyer, K. Hollingsworth, and P. Flynn. Image understanding for iris biometrics: a survey. *Journal of Computer Vision and Image Understanding*, 110(2):281–307, 2007.

	FRGC-1: neutral expression (different session)			*FRGC-2* : alternate expression (same session)			*FRGC-3*: alternate expression (different session)		
	Texture	Color	Texture + Color	Texture	Color	Texture + Color	Texture	Color	Texture + Color
left periocular	84.6	72.9	87.1	95.6	95.4	96.8	81.2	72.4	87.1
right periocular	87.1	76.3	88.3	95.6	96.1	96.8	83.4	74.2	87.1
left + right	91.5	82.9	**91.0**	97.6	97.6	**98.3**	88.8	82.0	**91.2**
face	94.6	63.2	91.7	98.8	92.2	98.8	90.7	52.4	85.1

Table 1. Rank - 1 recognition rate for the three FRGC experiments described in this paper.

[5] S. Crihalmeanu, A. Ross, and R. Derakhshani. Enhancement and registration schemes for matching conjunctival vasculature. *Proc. of the 3rd IAPR/IEEE International Conference on Biometrics (ICB)*, pages 1240–1249, 2009.

[6] J. Daugman. How iris recognition works. *IEEE Trans. on Circuits and Systems for Video Technology*, 16:21–30, 2004.

[7] H. K. Ekenel and R. Stiefelhagen. Generic versus salient region based partitioning for local appearance face recognition. In *IAPR/IEEE International Conference on Biometrics (ICB)*, 2009.

[8] B. Heisele, T. Serre, and T. Poggio. A component-based framework for face detection and identification. *International Journal of Computer Vision*, 74(2):167–181, 2007.

[9] P. Heisele, B.and Ho, J. Wu, and T. Poggio. Face recognition: component-based versus global approaches. *Computer Vision and Image Understanding*, 91((1-2)):6–21, 2003.

[10] A. K. Jain and U. Park. Facial marks: soft biometric for face recognition. In *Proceedings of the IEEE International Conference on Image Processing*, 2009.

[11] S. Z. Li, R. Chu, M. Ao, L. Zhang, and R. He. Highly accurate and fast face recognition using near infrared images. *Proc. Advances in Biometrics, International Conference, Lecture Notes in Computer Science 3832, Springer*, pages 151–158, 2006.

[12] S. Liao, W. Fan, A. Chung, and D. Yeung. Facial expression recognition using advanced local binary patterns, tsallis entropies and global appearance features. *Proc. of the IEEE International Conference on Image Processing (ICIP)*, pages 665–668, 2006.

[13] P. Miller, A. Rawls, S. Pundlik, and D. Woodard. Personal identification using periocular skin texture. In *ACM Symposium on Applied Computing*, 2009.

[14] T. Ojala, M. Pietik*äi*nen, and T. M*äe*np*ää*. Multiresolution gray-scale and rotation invariant texture classification with local binary patterns. *IEEE Transactions on Pattern Analysis and Machine Intelligence (PAMI)*, 24(7):971–987, 2002.

[15] U. Park, A. Ross, and A. K. Jain. Periocular biometrics in the visible spectrum: a feasibility study. In *Biometrics: Theory, Applications and Systems*, 2009.

[16] J. Philips. Multiple Biometrics Grand Challenge, http://face.nist.gov/mbgc/.

[17] P. J. Phillips, P. J. Flynn, T. Scruggs, K. W. Bowyer, J. Chang, K. Hoffman, J. Marques, J. Min, and W. Worek. Overview of face recognition grand challenge. *IEEE Conference on Computer Vision and Pattern Recognition*, 2005.

[18] M. Savvides, R. Abiantun, J. Heo, C. Xie, and B. K. Vijayakumar. Partial and holistic face recognition on frgc ii using support vector machines. *Proc. of IEEE Computer Vision Workshop (CVPW)*, page 48, 2006.

[19] P. Sinha, B. Balas, Y. Ostrovsky, and R. Russell. Face recognition by humans: Nineteen results all computer vision researchers should know about. *Proc. IEEE*, 94(11):1948–1962, November 2006.

[20] Z. Sun, T. Tan, and X. Qiu. Graph matching iris image blocks with local binary pattern. *Proc. Advances in Biometrics, International Conference (ICB), Lecture Notes in Computer Science 3832, Springer*, pages 366–373, 2006.

[21] M. A. Turk and A. P. Pentland. Face recognition using eigenfaces. In *Proceedings of the IEEE Conference on Computer Vision and Pattern Recognition*, pages 586–591, 1991.

[22] J. Wright, A. Yang, A. Ganesh, S. Sastry, and Y. Ma. Robust face recognition via sparse representation. *IEEE Transactions on Pattern Analysis and Machine Intelligence*, 31(2):210–227, Feb. 2009.

[23] W. Zhao, R. Chellappa, P. J. Phillips, and A. Rosenfeld. Face recognition: A literature survey. *ACM Comput. Surv.*, 35(4):399–458, 2003.